



Comparison of Electrophysiological and Radiological Subthalamic Nucleus Length and Volume

Bekir TUGCU¹, Ozan HASIMOGLU¹, Ayca ALTINKAYA², Ozan BARUT¹, Taha HANOGLU¹

¹University of Health Sciences, Hamidiye Faculty of Medicine, Basaksehir Cam and Sakura City Hospital, Department of Neurosurgery, Istanbul, Turkey

²University of Health Sciences, Hamidiye Faculty of Medicine, Basaksehir Cam and Sakura City Hospital, Department of Neurology, Istanbul, Turkey

Corresponding author: Bekir TUGCU ✉ tugcubekir@gmail.com

ABSTRACT

AIM: To investigate the surgical value of MER recordings and improve surgical technique by demonstrating the consistency between preoperative radiological STN volume and intraoperative neurophysiological STN length.

MATERIAL and METHODS: Sixty-one patients with PD were enrolled. The volumes of the STN were measured using magnetic resonance images 3-dimensional volume reconstructions of stereotactic magnetic resonance images. MER were performed in all patient and the maximal electrophysiologic length of the STN was recorded each patient. In the postoperative period, the permanent electrode was modeled and reconstructed in 3D, and the longest distance traveled in the STN was calculated.

RESULTS: A total of 61 patients who underwent surgery between 2012-2022 were included in the study. Thirty-six (59%) of the patients were male, and 25 (41%) were female. A total of 122 STNs were performed with 166 electrodes. The most common end alignment used was center with 86. STN length averaged 4.9 mm (0-10.5 mm). The mean STN volume was 0.11 cm³. The STN Volume of men were significantly higher than women. The STN Length, Volume, and the target MER length showed a positive correlation significantly.

CONCLUSION: With radiological advances, it is possible to better visualize the target points and define the boundaries better, and direct methods can be used more in making targeting plans. MER records obtained during surgery and STN dimensions in pre-surgical planning show compatibility, and it is seen that there may be differences between the right and left sides because of brain shifting. Although radiology is increasingly providing better support, electrophysiological recordings provides real-time information on the electrodes' locations and give the opportunity to surgical team choosing alternative target.

KEYWORDS: Subthalamic nucleus, Microelectrode recording, Parkinson's disease, Deep brain stimulation

ABBREVIATIONS: PD: Parkinson's disease, **SNpc:** Substantia nigra pars compacta, **LD:** Levodopa, **STN:** Subthalamic nucleus, **GPI:** Globus pallidus interna, **MRI:** Magnetic resonance imaging, **MER:** Microelectrode recording, **DBS:** Deep brain stimulation, **CT:** Computed tomography

■ INTRODUCTION

Parkinson's Disease (PD) is a chronic progressive neurodegenerative disease characterized by the early prominent death of dopaminergic neurons in the substantia nigra pars compacta (SNpc). PD is the second most common neurodegenerative disease after Alzheimer's Disease and its frequency has been increasing for the last three decades. PD prevalence is increasing with age and PD affects 1% of the population above 65 years (17). Dopamine deficiency in the basal ganglia causes the classic motor symptoms of PD such as bradykinesia, tremor, rigidity, and postural instability. In addition to motor symptoms, autonomic dysfunction and neurobehavioral problems are also seen. Levodopa (LD) is the main pharmacological treatment for PD. However, with the progression of the disease, LD response decreases, and LD-related dyskinesias begin to appear. Patients who cannot be treated with LD alone and are suitable for the surgical procedure can be operated on using the subthalamic nucleus (STN) and globus pallidus interna (GPI) as anatomical targets.

The STN is a basal ganglia structure that is subdivided into sensorimotor, limbic, and associative subdivisions according to the distribution of cortical projections (8,13). The dorsal part is under the control of the motor, and the ventral part is under the control of the limbic and associative systems. Most of the neurons originating from the STN are excitatory (glutamatergic) neurons and stimulate the GPI (7). GPI contains primarily inhibitory GABAergic neurons that project to the thalamus. And thalamus sends excitatory outputs to the cortex. STN plays a key role in the basal ganglia indirect pathway, which prevents unwanted movements by stimulating GPI. Stimulation of GABAergic neurons of the GPI results in decreased excitation of the thalamus and this leads to reduced movements (13). The medial portion of the STN also contains limbic connections with the nigral and ventral tegmental area. Because of these connections, chronic deep brain stimulation (DBS) in PD patients may cause symptoms related to the limbic system.

The STN is a small, biconvex and lens-shaped structure with a high functional capacity and is located at the intersection of important white matter pathways and close to important structures. For this reason, accurate determination of the position of the STN is very essential in surgical procedures. Small deviations in the position of the STN may cause side effects or unsuccessful surgeries. In DBS surgery, direct and indirect methods are used to determine the STN location where the electrodes will be placed. STN contains a high amount of iron and is therefore directly determined by high-resolution magnetic resonance imaging (MRI). Indirectly, the target is determined using stereotactic atlas coordinates. In the first method, there is a margin of error, since not all boundaries of the STN are always visible on MRI, while in the second method, the coordinates of the atlas are not the patient's STN coordinates. In addition, during surgery, there may be shifts in the coordinate plane due to reasons such as loss of cerebrospinal fluid (CSF), positional changes, and measurement techniques. For this reason, in most centers, the STN site is verified electrophysiologically for accurate

targeting. This process is called microelectrode recording (MER).

Our aim in this study was to compare the length and volume of the radiological STN with the length in the electrophysiologically mapped MER recordings. In addition, it will be investigated whether age and gender variables are related to STN length, volume, and MER length. This data will show us whether the electrophysiological borders taken in the MER are compatible with the STN in high-resolution MRI.

■ MATERIAL and METHODS

This study was approved by the local ethics committee (KAEK/2022.03.92). A total of 61 idiopathic PD (IPD) patients were included in this study. All patients underwent Subthalamic Nucleus Deep Brain Stimulation (STN-DBS) operation between 2012-2022. Demographic characteristics, clinical history, family history, UPDRS, Schwab and England, Hoehn & Yahr scores, psychiatric status, PDQ-39 scale, and on-off medication examinations of the patients were recorded. Based on this information, surgery was planned by the decision of the local movement disorder council (neurosurgeon, neurologist, psychiatrist, psychologist).

Imaging and Planning Protocols

All participants underwent MRI examination 1-3 days before surgery with turbo spin echo T1 (TR 1060 ms, TE Shortest ms, slice thickness 1 mm with no gaps, matrix 252 × 240 pixels), T2 (TR 2500 ms, TE: shortest 260 ms, slice thickness 1 mm with no gaps, matrix 252X252 pixels), sagittal and double-dose gadolinium-enhanced Turbo spin echo T1c (TR 1060 ms, TE shortest ms, slice thickness 1mm with no gaps. Matrix 252 x 240). All MRI scans were performed using a Philips MRI Ingenia 3.0 Tesla (Philips/Netherlands). The images were recorded parallel to the AC-PC line from the vertex to skull basis. The Integra CRW Stereotactic Frame (Integra, New Jersey, USA) or Leksell Frame (Elekta inc. Stockholm, Sweden) was mounted on the patients on the morning of the operation. Then, Computed Tomography (CT) was taken from the vertex to the base of the skull, showing the entire frame at 1 mm thickness (Healthcare Supria 64 Slice, Hitachi, Japan). We fused MRI and CT images via BrainLab Elements (Brainlab, Munich, Germany) software. We determined the AC-PC line and aimed indirectly at STN 12 mm lateral, 2 mm posterior, and 4 mm inferior to the mid-commissural point. Finally, we adjusted the trajectory and dorsolateral STN using T2 MR images directly. In addition, a CT image (1 mm thick) was taken 6 hours after surgery to confirm electrode placement and check complications.

Preoperative Planning and Surgery

All patients' medications were stopped 12 hours before the operation. Sedation was performed with remifentanyl hydrochloride and dexmedetomidine in the operating room. The sterile stereotactic frame was mounted to the patient's head after the sterile area was covered with the isolation drape. Afterward, Burr Hole points were determined and local anesthesia was provided with lidocaine hydrochloride. We usually start the

operation from the contralateral of the side where the findings are more severe. Often, the symptoms are more severe on the right side of patients. If symptoms are equal on both sides, left STN is preferred first. In this study, the first target was Left STN in all patients. After opening the Burr Hole, the Burr Hole cover was fixed to the bone. Then the MER probe was placed into the brain 10 mm above the target. Electrophysiological responses were recorded by moving the probe 1 mm at the first 5 mm distance and then 0.5 mm. MER regions compatible with STN were noted. When the STN signal was finished, the MER was completed and macro stimulation was applied from the regions with the best signal. After macro stimulation, the lead was placed where rigidity, bradykinesia, and tremor improved best and the side effects were the lowest. The same procedure was applied to the contralateral side. Finally, we placed the neuro-generator in the left pectoral area under general anesthesia and the operation was finalized.

Image Processing

After fusing the patients' T2w, T1, T1c, and postoperative CT images in the BrainLab Elements program, we calculated the borders and volumes of the STN by automatically segmenting the STN in the object segmentation module (14) (Figure 1). STN boundaries were checked on T2w images and were corrected in case of incorrect segmentation. We modeled the lead in 3D on the postoperative CT in the lead localizer

module. We selected the image which included the widest STN boundaries on the T2w image and accepted this as the starting point for the axis of the electrode. In that image, we plotted the length from the center of the electrode to the STN boundaries. We considered this length to be the STN length (Figure 2).

Electrophysiological Evaluation

In this study, we used insulated tube microelectrodes with 3-mm tungsten tips and 1.1-mm outer diameters in all patients. We placed the electrodes on the Ben-Gun in the "+" orientation. We used five Ben-Gun apparatus with a spacing of 2 mm for each electrode (Anterior, Posterior, Lateral, Medial, Centre) (2). We tracked the electrophysiological signals as tone and wave using the software (Alpha Omega MER system, Israel). We recorded the STN-registered regions in 0.5-mm increments. We accepted the electrophysiological recording interval of the STN verifiable by at least two observers and the software (11). We noted the length of this region separately for each STN and each anatomic orientation (Figure 3). The Ben-Gun alignment in which the lead electrode was placed was considered the target MER length.

Comparison of the Data

The relationship between target MER length and the STN volume and STN length as a function of age and gender was

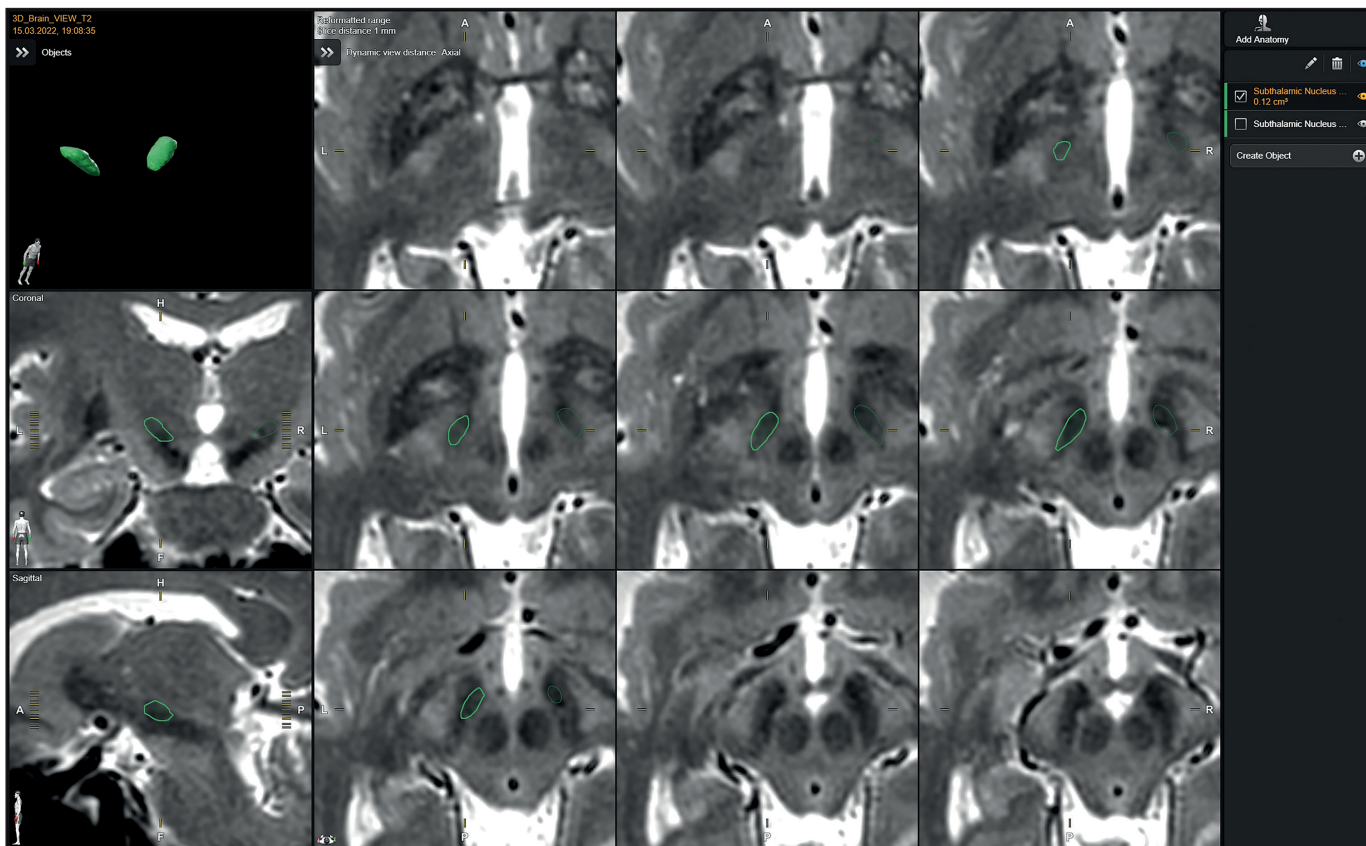


Figure 1: Segmentation of Left STN on T2 MR image. STN boundaries were determined in the automatic segmentation module of BrainLab elements software. Afterward, the errors were fixed manually. Finally, the STN volume was recorded.

first examined for both STNs and then for the left and right STNs separately. Then, we compared STN length with target MER records from the final Ben-Gun alignment. Finally, we compared STN volume separately with all MER records from the available orientations.

Exclusion Criteria

Of the 99 patients who underwent surgery between 2012 and 2022 STN-DBS, patients whose data were not regularly retained, MER records could not be obtained for technical reasons, and those with damaged or missing radiological images were excluded from the study.

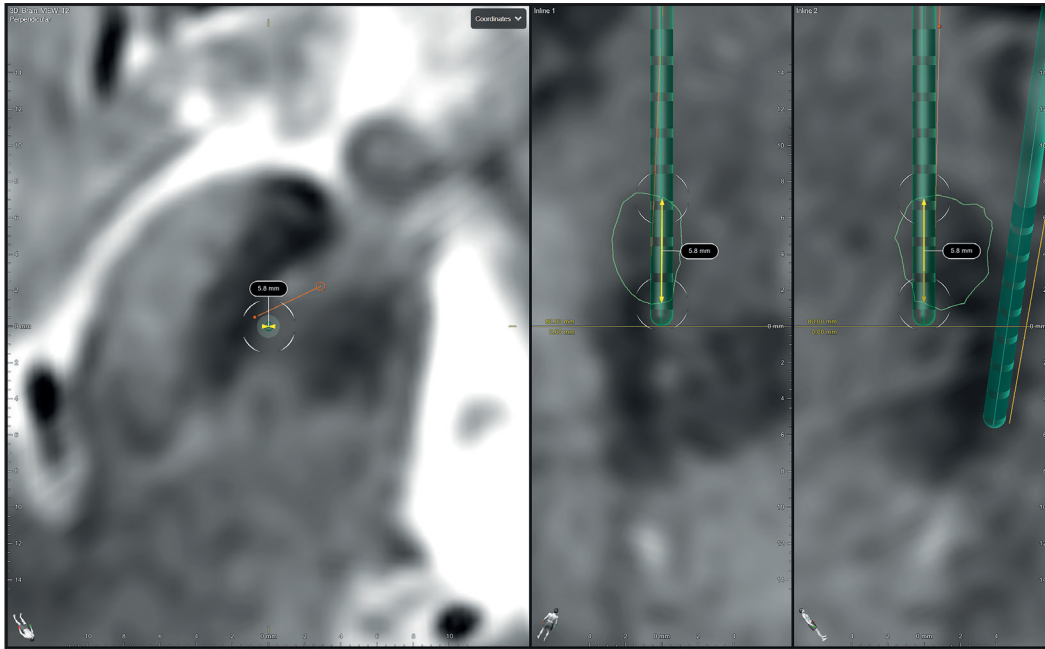


Figure 2: Measurement of the length of the Left STN on the T2 MR image. The lead was modeled in 3D on the postoperative CT. Then, the 3D lead was fused to the T2-weighted image. The image was reconstructed with the lead as the axis. The widest view of the demarcated STN was selected (Green). Finally, the length of the STN was measured along the midline of the lead (Yellow).

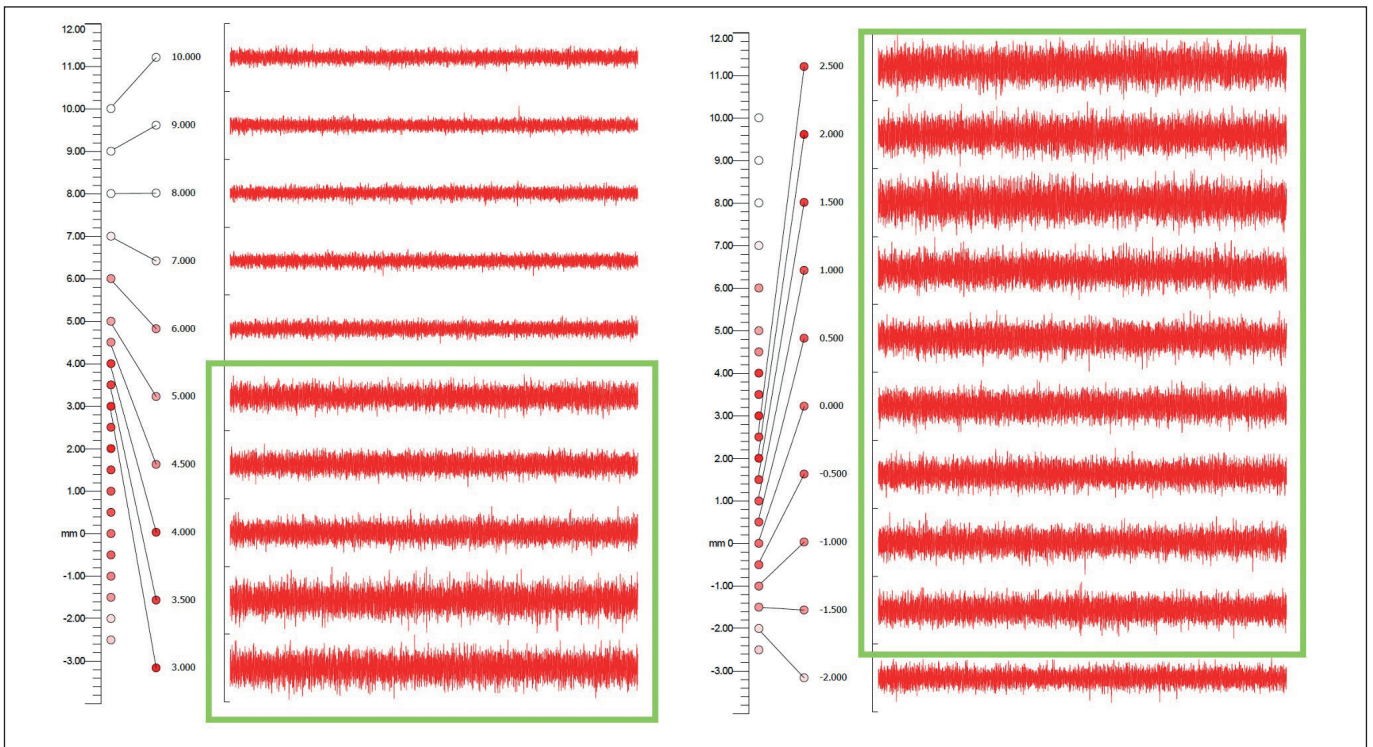


Figure 3: Example of a MER, MER shows STN length. The MER area coherent with the STN is shown in the green square.

Statistical Analysis

We analyzed the data using the SPSS 22 program. We analyzed the radiographic length and volume values of the STN and the MER length values in terms of skewness-kurtosis and decided to use nonparametric tests. We used the Mann-Whitney U-Test of the comparisons for two separate groups, Spearman Correlation Analysis for relational analysis, and the Wilcoxon Signed Rank Test for tests with dependent samples. The confidence interval was set at 95% (p=0.05).

RESULTS

Comparison of Demographic Characteristics

Sixty-one patients (122 STNs) who underwent surgery between 2012-2022 were included in the study. Thirty-six (59%) of the patients were male, and 25 (41%) were female. The mean age was 54.91 years (34-70 ± 8.92). We used a total of 166 electrodes. We used an average of 2.67 (1-5) electrodes. The most common electrode orientation used was center with 86 (center (86), anterior (20), lateral (5), medial (9), and posterior (2)). The mean STN length was 4.9 mm (0-10.5 mm). The mean STN volume was 0.11 cm³ (0.09-0.14 cm³).

The correlation between the age of the patients and whole STN Length (n=122), Volume, and the target MER length values were analyzed with Spearman Correlation Analysis. There was no significant correlation between the ages and values (p>0.05).

The Mann-Whitney U Test was applied to determine the differences between genders for STN Length, Volume, and target MER values. The STN volumes of men were significantly higher than those of women (p<0.05), and there was no significant difference in other comparisons (Table I).

The relationship between the age of the patients and right and left STN Length, Volume, and the target MER length values were analyzed separately by Spearman Correlation Analysis. There was no significant correlation between the ages and values (p>0.05).

The Mann-Whitney U-Test was applied to determine the differences between genders for the right and left STN Length, Volume, and target MER values separately. The right and left STN Volume values of men were higher than those of women at significant levels (p<0.01). However, STN Length values and highest target MER values did not differ between men and women (p>0.05) (Table II).

Comparison of Radiological Data and Electrophysiological Data

Spearman Correlation Analysis was applied to determine the relationship between 122 STN Length, Volume, and target MER length values. The STN Length, Volume, and the target MER length showed a significant positive correlation (p<0.05) (Table III).

Wilcoxon Signed Rank Non-parametric Test was applied to compare the right and left STN Length and target MER values.

Table I: Relationship Between STN Length, Volume, Target MER Length and Gender Length

	Avg	SD	p
STN length			
Male	4.933	0.965	0.340
Female	4.830	1.333	
STN Volume			
Male	0.115	0.014	0.001*
Female	0.097	0.010	
MER (Target)			
Male	5.416	1.609	0.983
Female	5.310	1.551	

*SD: Standard Deviation, *p: Mann-Whitney U significance level.*

Table II: Comparison of Right and Left STN Lengths and Volumes by Gender

	Gender	n	Avg.	SD	p
L STN Length	Male	36	4.958	0.753	0.691
	Female	25	4.872	0.864	
L STN Volume	Male	36	0.115	0.015	<0.000
	Female	25	0.098	0.010	
R STN Length	Male	36	4.908	1.148	0.347
	Female	25	4.788	1.696	
R STN Volume	Male	36	0.115	0.014	<0.000
	Female	25	0.096	0.011	
L MER (target)	Male	36	5.333	1.558	0.695
	Female	25	5.360	1.747	
R MER (target)	Male	36	5.500	1.677	0.980
	Female	25	5.260	1.362	

SD: Standard Deviation, p: Mann-Whitney U Test.

Table III: Relationship Between STN Length, Volume, and Target MER Length

	r	STN length	STN Volume	MER (Target)
STN Length	r	1		
	p	.		
STN Volume	r	0.373	1	
	p	0.000*	.	
MER (Target)	r	0.034	0.025	1
	p	0.03*	0.032*	.

p<.05, N: 122, r: Spearman Correlation Coefficient.

STN Length of the left side was significantly lower than the MER values ($p < 0.05$). There was no significant difference for the values of the right side ($p > 0.05$) (Table IV).

The Spearman Correlation Analysis was applied to investigate the relationship between STN Volume values and all MER values. There was a positive correlation for all MER orientations

Table IV: Comparison of Right and Left STN Lengths and Target MER Lengths

	Avg.	SD	p
L STN Length	4.923	0.102	<0.017*
L MER (target)	5.344	0.208	
R STN Length	4.859	0.178	0.083
R MER (target)	5.401	0.198	

*SD: Standard Deviation, N: 61, *p: Wilcoxon Signed Rank Test.*

Table V: Comparison of Right and Left STN Volumes and MER Lengths

	n	Avg.	SD	p	
Left	STN Volume	60	0.108	0.0157	0.000*
	Center	60	4.575	2.164	
	STN Volume	36	0.106	0.0136	0.000*
	Anterior	36	2.791	2.287	
	STN Volume	27	0.109	0.0153	0.000*
	Lateral	27	3.148	2.065	
	STN Volume	19	0.104	0.0146	0.003
	Medial	19	3.421	2.714	
	STN Volume	17	0.103	0.0145	0.013
	Posterior	17	1.823	2.404	
Right	STN Volume	59	0.108	0.0158	0.000*
	Center	59	4.389	2.343	
	STN Volume	36	0.107	0.0144	0.000*
	Anterior	36	3.333	2.501	
	STN Volume	25	0.107	0.0130	0.001
	Lateral	25	2.380	2.052	
	STN Volume	25	0.105	0.0155	0.002
	Medial	25	3.000	2.780	
	STN Volume	18	0.104	0.0142	0.013
	Posterior	18	2.000	2.294	

*SD: Standard Deviation, *p: Wilcoxon signed rank test.*

($p < 0.05$). When the right and left STN volumes and MER values were compared separately, there was a positive correlation for all MER orientations ($p < 0.05$) (Table V).

DISCUSSION

The exact detection of the correct target point defines the most critical point of the operation in neuromodulation surgeries for movement disorders. For PD, the primary goal is to confirm the location of the STN and its borders, especially the lateral and dorsal parts. The main purpose is not only to obtain a maximum motor response to determine the motor component of STN exactly but also to avoid complications because of electrodes close to the corticospinal tract, medial lemniscus, and oculomotor fibers. Small deviations in the determination of the STN location can result in undesirable side effects or unsuccessful surgeries. The first step in determining the target point is to make a radiologically correct calculation. Although the radiological determination of STN borders can be done better with the development of MR imaging, it is a common surgical technique to verify the possible shift or margin of error during the operation with other methods like neurophysiological evaluation (4,6,9,10,12,15,16).

It is possible to use neurophysiological refinement to determine the location and size of the STN. At the same time, using intraoperative macro stimulation provides the opportunity to determine the correct target point and to detect important adjacent anatomical structures that may cause possible side effects (9,10,12,15). The most important monitored values during neurophysiological recording are changes in background activities and frequency changes of cell discharges. Simultaneous evaluation of both visual and auditory data is essential in monitoring these changes. It is essential for optimal electrode placement that the DBS electrode travels the longest STN line possible while passing through the motor component within the STN. It is possible to determine the length of the STN dimensions along the trajectory by detecting the input and output characteristic data to the STN with visual and audio data. Rapid persistent increase in background activity is a characteristic entrance indicator to STN. On the other hand, a rapid decrease in background activity accompanying regular and high-frequency cell discharges is characteristic of the SNr penetration after the ventral border of the STN. It is possible to use some quantitative data from MER (15,19). The severity of PD is directly correlated with the volumetric number of cells that are degenerated and lost (5). Therefore, the firing frequency of cells will be quantitatively different in patients with severe PD accompanied by more cell loss. Using quantitative parameters will provide additional information for a more precise determination of STN location.

There are studies investigating the compatibility of radiological STN length according to MR images with MER. In our study, the radiological length and volume of the STN were calculated with the assistance of Artificial Intelligence and its relationship with MER was investigated (3,10,12,15,16). STN size and volume were found to be correlated, with males significantly larger volumes of STN than females. When the literature was reviewed, it was seen that there is no consensus on this issue,

on the contrary, there is a publication reporting significantly larger STN volume in women (21).

Our results revealed that the radiological size and volume of the STN obtained from MR images are similar to the electrophysiological size obtained in the intraoperative recording. When the right and left STN lengths and the target MER length were evaluated separately, the target MER length was higher on the left side. The first target point was the left STN in all patients included in the study. In this case, shift causes such as CSF leakage and pneumocephalus are more likely to be seen on the right side. Therefore, we think that the higher target MER length compared to the left STN length is due to the lower shift effect.

It was correlated with the volume measurements created by Artificial Intelligence and the recording data obtained from the most used centrally placed electrode. In our study, the least preferred recording electrode was the posterior one located one in 35 cases. Other preferred electrode recordings were anterior, lateral, and medial electrodes, respectively, with electrophysiological data consistent with STN volume measurements.

CONCLUSION

After the developments in MRI techniques and combination with very advanced computer software, indirect targeting methods are gradually abandoned and direct targeting methods are used more and more. The results of our study show that electrophysiological data and preoperative radiological targeting are compatible. We consider electrophysiological data are still valuable because the relationship between STN lengths and MER values differs between right and left. Considering the publications that the use of MER is associated with higher infection rates, more intracerebral hemorrhage, and prolonged operation time, it can be argued that DBS surgery without the use of MER with direct targeting can be reliable. However, there will only be a chance of stimulation through the center electrode, and if unexpected side effects are observed, it will be difficult to evaluate the possible second choice electrode (1,18,20). However, when this happens, the second lead with good neurophysiological data can be stimulated to be selected for the permanent electrode site using MER.

AUTHORSHIP CONTRIBUTION

Study conception and design: BT, OH

Data collection: BT, OH, TH

Analysis and interpretation of results: AA, OB

Draft manuscript preparation: BT, OH

Critical revision of the article: BT, OH

All authors (BT, OH, AA, OB, TH) reviewed the results and approved the final version of the manuscript.

REFERENCES

- Binder DK, Rau GM, Starr PA: Risk factors for hemorrhage during microelectrode-guided deep brain stimulator implantation for movement disorders. *Neurosurgery* 56:722-732, 2005
- Bus S, Pal G, Ouyang B, van den Munckhof P, Bot M, Sani S, Metman LV: Accuracy of microelectrode trajectory adjustments during DBS assessed by intraoperative CT. *Stereotact Funct Neurosurg* 96:231-238, 2018
- Bus S, van den Munckhof P, Bot M, Pal G, Ouyang B, Sani S, Verhagen Metman L: Borders of STN determined by MRI versus the electrophysiological STN. A comparison using intraoperative CT. *Acta Neurochir* 160:373-383, 2018
- Chau AM, Jacques A, Lind CR: Defining the border of the subthalamic nucleus for deep brain stimulation: A proposed model using the symmetrical sigmoid curve function. *World Neurosurg* 143:e567-e573, 2020
- Colpan ME, Slavin KV: Subthalamic and red nucleus volumes in patients with Parkinson's disease: Do they change with disease progression? *Parkinsonism Relat Disord* 16:398-403, 2010
- Duchin Y, Shamir RR, Patriat R, Kim J, Vitek JL, Sapiro G, Harel N: Patient-specific anatomical model for deep brain stimulation based on 7 Tesla MRI. *PLoS one* 13:e0201469, 2018
- Haber SN: Corticostriatal circuitry. *Dialogues Clin Neurosci* 18(1):7-21, 2016
- Haynes WI, Haber SN: The organization of prefrontal-subthalamic inputs in primates provides an anatomical substrate for both functional specificity and integration: Implications for Basal Ganglia models and deep brain stimulation. *J Neurosci* 33:4804-4814, 2013
- Horn A, Kühn AA, Merkl A, Shih L, Alterman R, Fox M: Probabilistic conversion of neurosurgical DBS electrode coordinates into MNI space. *Neuroimage* 150:395-404, 2017
- Kocabicak E, Aygun D, Ozaydin I, Jahanshahi A, Musa O, Omer B, Murat K, Hatice G, Terzi M, Alptekin O: Does probe's eye subthalamic nucleus length on T2W MRI correspond with microelectrode recording in patients with deep brain stimulation for advanced Parkinson's disease? *Turk Neurosurg* 23(5):658-665, 2013
- Lozano CS, Ranjan M, Boutet A, Xu DS, Kucharczyk W, Fasano A, Lozano AM: Imaging alone versus microelectrode recording-guided targeting of the STN in patients with Parkinson's disease. *J Neurosurg* 130:1847-1852, 2018
- Nowacki A, Nguyen TK, Tinkhauser G, Petermann K, Debove I, Wiest R, Pollo C: Accuracy of different three-dimensional subcortical human brain atlases for DBS-lead localisation. *Neuroimage Clin* 20:868-874, 2018
- Parent A, Hazrati LN: Functional anatomy of the basal ganglia. I. The cortico-basal ganglia-thalamo-cortical loop. *Brain Res Brain Res Rev* 20:91-127, 1995
- Reinacher PC, Várkuti B, Krüger MT, Piroth T, Egger K, Roelz R, Coenen VA: Automatic segmentation of the subthalamic nucleus: A viable option to support planning and visualization of patient-specific targeting in deep brain stimulation. *Oper Neurosurg* 17:497-502, 2019

15. Schlaier JR, Habermeyer C, Warnat J, Lange M, Janzen A, Hochreiter A, Proescholdt M, Brawanski A, Fellner C: Discrepancies between the MRI-and the electrophysiologically defined subthalamic nucleus. *Acta Neurochir* 153:2307-2318, 2011
16. Sterio D, Zonenshayn M, Mogilner AY, Rezai AR, Kiprovski K, Kelly PJ, Beric A: Neurophysiological refinement of subthalamic nucleus targeting. *Neurosurg* 50:58-69, 2002
17. Tanner CM, Goldman SM: Epidemiology of Parkinson's disease. *Neurol Clin* 14:317-335, 1996
18. Temel Y, Wilbrink P, Duits A, Boon P, Tromp S, Ackermans L, van Kranen-Mastenbroek V, Weber W, Visser-Vandewalle V: Single electrode and multiple electrode guided electrical stimulation of the subthalamic nucleus in advanced Parkinson's disease. *Oper Neurosurg* 61:ONS346-ONS357, 2007
19. Verhagen R, Zwartjes DG, Heida T, Wiegers EC, Contarino MF, de Bie RM, van den Munckhof P, Schuurman PR, Veltink PH, Bour LJ: Advanced target identification in STN-DBS with beta power of combined local field potentials and spiking activity. *J Neurosci Methods* 253:116-125, 2015
20. Xiaowu H, Xiufeng J, Xiaoping Z, Bin H, Laixing W, Yiqun C, Jinchuan L, Aiguo J, Jianmin L: Risks of intracranial hemorrhage in patients with Parkinson's disease receiving deep brain stimulation and ablation. *Parkinsonism Relat Disord* 16:96-100, 2010
21. Zwirner J, Möbius D, Bechmann I, Arendt T, Hoffmann KT, Jäger C, Lobsien D, Möbius R, Planitzer U, Winkler D: Subthalamic nucleus volumes are highly consistent but decrease age-dependently-a combined magnetic resonance imaging and stereology approach in humans. *Human Brain Mapp* 38:909-922, 2017